Bench-scale study of ultrafiltration membranes for evaluating membrane performance in surface water treatment

Dillon A. Waterman, Steven Walker, Bingjie Xu and Roberto M. Narbaitz

ABSTRACT

Currently, there is no standard bench-scale dead-end ultrafiltration (UF) testing system. The aim of the present study was to design and build a bench-scale hollow fiber UF system to assess the impact of operational parameters on membrane performance and fouling. A bench-scale hollow fiber UF system was built to operate at a constant flux (±2% of the set-point flux) and included automated backwash cycles. The development of the bench-scale system showed that it is very difficult to maintain a constant flux during the first minute of the filtration cycles, that digital flow meters are problematic, and that the volume of the backwash waste lines should be minimized. The system was evaluated with Ottawa River water, which has a relatively high hydrophobic natural organic matter content and is typical of Northern Canadian waters. The testing using different permeate fluxes, filtration cycle duration and backwash cycle duration showed that this system mimics the performance of larger systems and may be used to assess the impact of operating conditions on membrane fouling and alternative pretreatment options. Modeling the first, middle, and last filtration cycles of the six runs using single and dual blocking mechanisms yielded inconsistent results regarding the controlling fouling mechanisms.

Key words | backwashing, bench-scale test, blocking law modeling, membrane fouling, ultrafiltration

Dillon A. Waterman
Steven Walker
Bingjie Xu
Roberto M. Narbaitz (corresponding author)
Department of Civil Engineering,
University of Ottawa,
161 Louis Pasteur,
Ottawa,
Ontario,
Canada K1N 6N5
E-mail: *narbaitz@uottawa.ca*

INTRODUCTION

New regulations regarding filtration, disinfection, and disinfection by-products (DBPs) have resulted in extensive growth in the use of hollow fiber membrane processes for drinking water treatment (MWH 2005; Yu & Graham 2015). Membrane processes are used to remove bacteria, protozoa, particles, hardness, dissolved salts, and natural organic matter (NOM), the latter being precursors to DBPs. In spite of the many advantages of membrane processes for drinking water treatment applications, there are concerns regarding membrane fouling, that is to say the increase in pressure or a reduction of permeate flux, through the accumulation of the particles on the membrane or within the membrane pores. Fouling can be minimized by the selection of more fouling resistant membranes, frequent backwashing, regular chemical cleaning, and optimized pretreatment (Wray *et al.* 2014; Touffet *et al.* 2015). Membrane fouling is caused by suspended particles, microorganisms, inorganic precipitates, and organic molecules (e.g., humic substances) (Nakatsuka *et al.* 1996; Yin *et al.* 2015). Current understanding of fouling is not sufficient for predicting fouling in dead-end ultrafiltration (UF) systems based on the measured water quality parameters and the membrane properties. Fouling rates are also significantly impacted by the nature of the foulant and the foulant–membrane interactions (Heijman *et al.* 2005). Pilot-scale testing is typically used to determine the treatability of a particular water source, membrane and system selection and to identify suitable operating conditions prior to design. These tests require one or more months and they are costly; they are often only possible when the supplier pays the expenses.

doi: 10.2166/wqrjc.2016.039

Pilot-plant studies simulate full-operation well but they are not very suitable for systematic investigations (Kim & DiGiano 2006). Bench-scale systems, if properly designed, can be a valuable tool in evaluating fouling and predicting the behavior of large-scale dead-end UF plants (Heijman *et al.* 2005). Bench-scale testing of competing membranes, alternative pretreatment processes, and operational regimes are more economical than pilot-scale testing and can economically be used to evaluate more alternatives. Most bench-scale membrane systems in the literature operate at a constant pressure and usually do not include a backwash cycle. In contrast, most full-scale membrane water treatment systems use hollow fibers, operate at a constant flux, and use frequent backwashes. Currently, there is no recognized standard bench-scale hollow fiber system or procedure. The objectives of this study were to design and build a bench-scale hollow fiber UF system and to demonstrate its capabilities by testing with a typical Northern Canadian water. The testing consists of: (1) exploring the effects of operational parameters, such as filtration time (FT), backwash time (BWT), and operating fluxes, on membrane performance; and (2) examining the effect of pretreatment on membrane performance. Although others have built similar testing apparatus, there is no standard bench-scale hollow fiber membrane testing apparatus and there are a number of potential problems/issues with these systems. In addition, this type of system has not been used to treat this particular highly colored river water, which has a high NOM content and a large hydrophobic NOM fraction, and is typical of Northern Canadian waters. The fouling data will be modeled to possibly gain insight on the dominant fouling mechanisms.

MATERIALS AND METHODS

Source water

The water selected for this research is Ottawa River water (ORW) which is rich in NOM, but has low turbidity, hardness, and alkalinity; NOM therefore is expected to be the main foulant. Several studies have determined that one of the most important foulants in drinking water treatment is NOM (Zularisam *et al.* 2006). Samples were collected at the Britannia Water Purification Plant which supplies water to the city of Ottawa, Ontario, Canada. The tests used raw water to accelerate the rate of fouling, which should show more clearly the impact of the process variables. NOM-rich waters like ORW would generally be pretreated by coagulation and sedimentation.

Membrane and module configuration

The membrane fibers used in this research are UltraPES 0.7 hollow fibers donated by Membrana, Germany. The membrane material is polyethersulfone with a nominal molecular weight cut-off (MWCO) of 70 kDa. The fibers have an internal diameter of 0.7 mm and outside diameter of 1 mm.

The membrane modules were constructed using 12.7 mm (½ inch) O.D. acrylic tubing (6.35 mm (¼ in) I.D.) capped at both ends with 12.7 mm (½ in) compression brass caps. Eight UF hollow fibers were placed within each module and then sealed at both ends with epoxy resin which hardened in 30 min. The eight 26 cm-long fibers provided a total surface area of 0.0046 m^2. The module is configured to operate in the inside-out dead-end mode by cutting one of the epoxy bulkheads to permit the feed to flow inside the fibers.

UF system design and set-up

Figure 1 depicts the UF system layout used in this research. The system was designed to replicate the filtration and backwash cycles of the full-scale membrane filtration operation.

The filtration side of the system (shown with solid lines in Figure 1) comprised a high performance peristaltic pump (EW-77250-62, Cole-Parmer, Montreal, QC), a low-profile in-line strainer system with a 178 μm mesh (K-29595-35, Cole-Parmer), a gate valve, an inlet pressure gauge, a pressure transducer, a three-way solenoid valve at the base of the membrane module, the membrane module, a two-way solenoid valve on the permeate side of the module, and a digital flowmeter (L-20CCM-D, Alicat Scientific, Tucson, AZ). The permeate was collected in beakers placed on a top-loading balance (K-11018-12, Cole-Parmer). The filtration side of the system was operated in the manual mode of the controller (i.e., feed is based on a percentage of pump output). The system maintained a

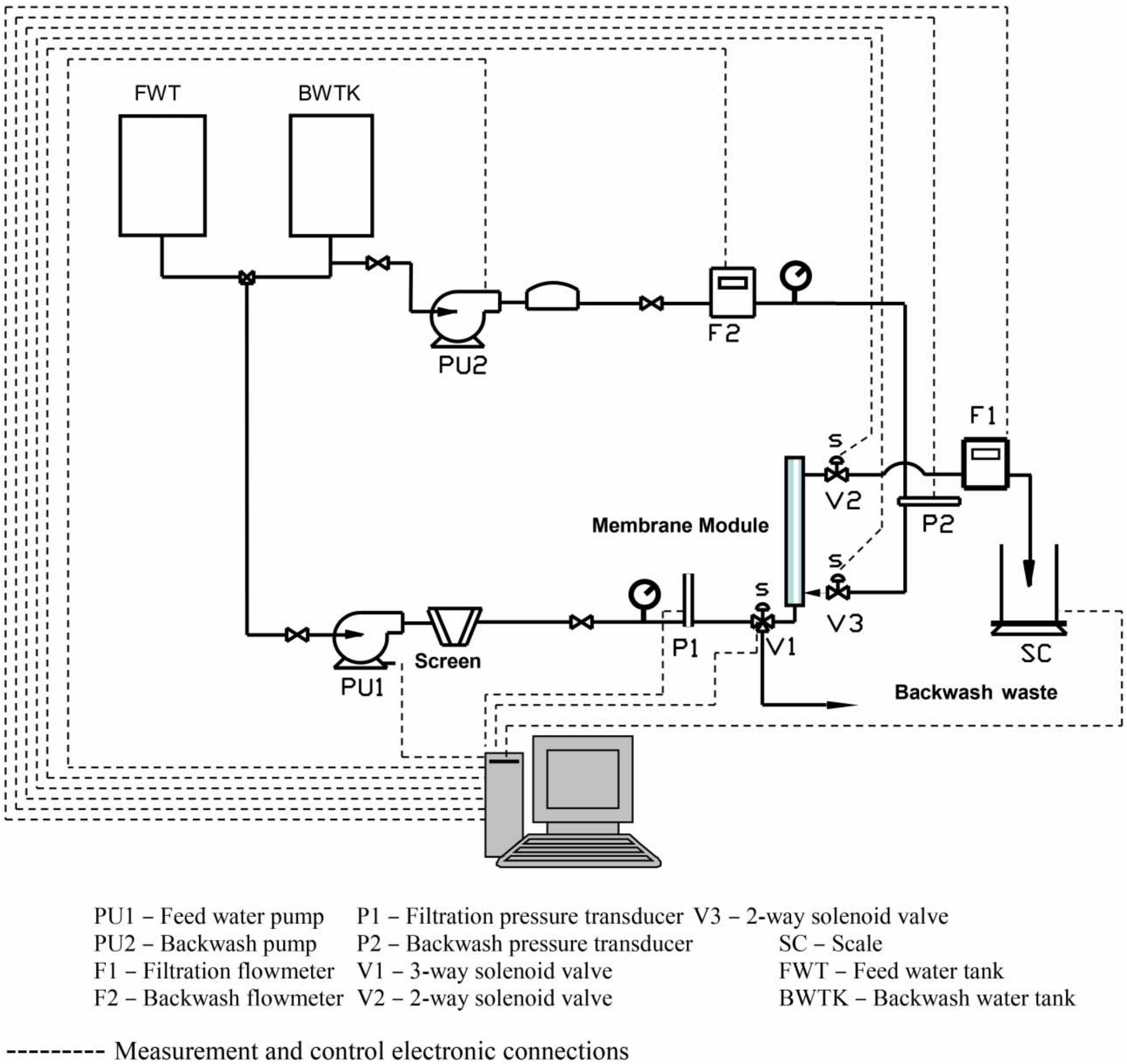

Figure 1 | The UF bench-scale system designed for this research.

constant flux within ±2% of the set-point flux. The filtration cycles proceed at constant flux until the preset FT was completed or the maximum allowable back pressure stipulated by the membrane manufacturer was reached, then the controller initiated the system backwash.

The backwash system was composed of a high pressure peristaltic pump (FPUDVS2007, Omega, Laval, QC), a pulsation dampener (EW-30610-37, Cole-Parmer) to smooth out flow variations produced by the peristaltic pump, a digital flowmeter (0–50 mL) (L-50CCM-D, Alicat Scientific), an inlet pressure gauge, a pressure transducer, and a two-way solenoid valve at the entrance to the shell side of the membrane module. The backwashing process utilized a controller and operates at constant flux.

The UF system shown in Figure 1 was operated and controlled with a LabVIEW interface (LabVIEW 8.5, National Instruments, Austin, TX). This program enabled the input of operating parameters including feed flowrate, filtration cycle length, water temperature, backwash flowrate, BWT, maximum operating pressure, the incremental increase/decrease of pump voltage based on the difference between actual and set flux, membrane radius, membrane length, the number of membrane fibers. The UF system was automated with a computer initiating both filtration and backwash cycles, through the starting and stopping of the feed water pump and the backwash pump, and through the opening and closing of the three solenoid valves. The system was complemented with a data acquisition system which recorded the major process outputs including operating time, flowrates, transmembrane pressures (TMPs) for feed and backwash cycles. The temperature (used in the empirical density relationship) was measured using a thermocouple (Digi-sense Thermocouple thermometer, C-91100-20, Cole-Parmer).

UF experiments

The filtration experiments consisted of three different stages. The first stage involved the preparation and configuration of the module as described in the section 'Membrane and module configuration'. A new module was constructed for each experiment. The second stage involved conditioning the membrane by pumping water through the module for an hour. Water produced by a Milli-Q system (Millipore, Bedford, MA) was used as the feed for these filtration tests.

The third stage examined the effect of operating parameters and pretreament on membrane performance. The first subset of 7-hour filtration experiments was conducted at a constant permeate flux of 100 L/m^{2}h with different FT of 15, 30, or 60 minutes treating raw ORW. Each filtration cycle was followed by a 1 or 2 minute-long backwashing cycle. The second subset of raw ORW filtration experiments evaluated the effect of different operating fluxes on membrane performance. Filtration experiments were performed at constant permeate flux values of 50, 70, and 100 L/m^{2}h, FT of 30 minutes and BWT of 1 minute. To assess the impact of pretreatment, the third subset of tests treated raw ORW and a sample of ORW which had been pretreated by alum coagulation, flocculation, and sedimentation. For these tests the system was operated at a permeate flux of 100 L/m^{2}h, a FT of 60 minutes, and a BWT of 1 minute. At the beginning of each experiment, Milli-Q water was used to stabilize the system before switching to river water. The filtration experiments were conducted in duplicate. Due to the limited volume of filtrate generated, the backwashings were performed with Milli-Q water.

Sample collection and analytical methods

Water from the intake of the water purification plant was collected and stored at 4 °C to retard biological degradation. The water was transferred to the laboratory and allowed to reach room temperature (20 °C) before the filtration test. Selected chemical and physical characteristics of the source water were determined using *Standard Methods* (APHA *et al.* 1998). Source water turbidity, pH, total organic matter (TOC), and ultraviolet absorbance at 254 nm (UV-254) were measured before each filtration test. TOC concentration, which was used as a surrogate for NOM concentration, was measured using an UV-persulfate oxidation-based TOC analyzer (Model 14-7045-000, Phoenix 8000, Tekmar Dohrmann, Cincinnati, OH). Three measurements were conducted for each sample with the standard deviation in each case <0.05 mg/L. UV-254, a useful indicator for humic substances, was measured using a Beckman DU-40 spectrophotometer. A 10 mm quartz cell was used to perform the measurements which were conducted in triplicate. The color of the raw water samples were ascertained using a color comparator (Aqua Tester by Orbeco Analytical Systems Inc., Farmingdale, NY). The pH of the samples was measured using a pH meter (Pinnacle 540, Corning, Lowell, MA). Turbidity was determined with a nephlometric turbidity meter (HACH 2100AN, Loveland, CO). Alkalinity was determined by titration with H_2SO_4, and hardness was calculated from titrations with EDTA (APHA *et al.* 1998).

Evaluation of process parameters and membrane performance

All experiments were analyzed on a dimensionless basis to compare multiple data sets obtained under various experimental conditions. The two main parameters used for evaluating membrane performance throughout this study were normalized specific flux (J_{NSF}) and backwash efficiency (η).

TMP for dead-end filtration was calculated as follows:

$$TMP = P_{in} - P_p \quad (1)$$

where P_{in} is the pressure at the inlet to the module (kPa) and

P_p is the permeate pressure (kPa) (MWH 2005). During this experiment the UF module discharged to the atmosphere, and so the TMP was equal to the gauge pressure at the inlet to the module. Under constant permeate flux (J) conditions, the fouling rate is observed by the decline in normalized specific flux (J_{NSF}), calculated as follows:

$$J_{NSF} = \frac{J/TMP}{J/TMP_0} = \frac{TMP_0}{TMP} \tag{2}$$

where J is the constant operating flux (L/m^{2}h), TMP_0 is the initial transmembrane pressure (kPa), and TMP is the transmembrane pressure (kPa) at any given time during the experiment (Kim & DiGiano 2006).

The backwash efficiency (η) was estimated as follows:

$$\eta = 100\frac{TMP_f - TMP_n}{TMP_f - TMP_i} \tag{3}$$

where TMP_f is the final TMP at the end of the filtration cycle, TMP_i is the initial TMP at the start of the same filtration cycle and TMP_n is the TMP following a backwash (Chellam et al. 1998).

The fraction of NOM removed from the permeate stream (rejection) was calculated as follows:

$$R = 1 - \frac{C_P}{C_F} \tag{4}$$

where R is rejection (dimensionless), C_P is the permeate TOC concentration (mg/L), and C_F is the feed water TOC concentration (mg/L) (MWH 2005).

RESULTS AND DISCUSSION

System construction and trouble shooting

Once the system was assembled, the electronic flowmeters caused significant difficulties in maintaining a constant permeate flux. They were very susceptible to interference by bubbles, which were frequently generated by the switching of the solenoid valves terminating backwashing and starting a new filtration cycle. Meter repositioning, as suggested by the manufacturer, did not solve the problem. Several alternative computer control schemes were evaluated to compensate for the problem, but the results were not satisfactory. The feed pump was changed to a more powerful peristaltic model and in conjunction with the above control system, it permitted the system to operate at a constant flux ±2% of the set-point flux. This level of flow variability is lower than those observed in many similar systems presented in the literature, but it was only achieved through a great deal of adjustment to the computerized control scheme. The use of electronic flowmeters is not recommended for this type of application.

Other interesting considerations in the design of the systems were related to the effectiveness of the backwashing in removing the accumulated foulant from the module and the system. The initial waste piping was unnecessarily long and appeared to lead to some carryover into the next filtration cycle. The effectiveness of the backwash depends on the backwash flow pattern within the module and the volume of water used in the backwashing. The role of the module geometry on backwash efficiency is an area that requires further research. Based on the TMP versus time patterns, the module design in the current study worked well. However, these modules had to be machined and were only used for one set of tests. Accordingly, alternative designs should be considered.

Securing hollow fibers for this type of test is challenging, as many manufacturers of membrane systems require a consent to publish agreement before donating or selling membrane fibers to researchers. This was not the case for the membranes used in this study. Another experimental challenge encountered was the removal of the membrane preservation agent in the membrane's fibers provided by a second supplier. Many attempts to remove this agent were unsuccessful, so testing was limited to a single type of membrane.

Water quality characteristics

The characteristics of the source water (ORW) and pretreated ORW are presented in Table 1. ORW has a light yellow-brown color, with low hardness and alkalinity. The color arises from the presence of NOM in the water (TOC = 5.80 ± 0.21 mg/L; UVA_{254} = 0.255 ± 0.018 cm^{-1}). For the duration of the experimental work, ORW had a turbidity of

Table 1 | Raw water quality of ORW

Parameter	Raw water	Coagulated and settled water
pH	7.49 ± 0.16	6.23 ± 0.1
Turbidity (NTU)	2.41 ± 0.26	0.706 ± 0.1
Alkalinity (mg/L as $CaCO_3$)	54	10
TOC (mg/L)	5.8 ± 0.205	2.81 ± 0.05
UV_{254} absorbance (cm^{-1})	0.255 ± 0.018	0.062 ± 0.015
SUVA $(L/mg\text{-}m)^{-1}$	4.40	2.21

2.41 ± 0.26 NTU and pH of 7.49 ± 0.16. Earlier fractionation studies have shown that only 1 to 8% of ORW NOM had molecular weights larger than 30,000 daltons (Jacangelo *et al.* 1994; Mosqueda-Jimenez *et al.* 2004; Nguyen *et al.* 2007). Given that the membranes in the current study have a nominal MWCO of 70 kDa and assuming size exclusion controls the NOM removal, the percent NOM removals were expected to be low.

XAD4 and XAD8 resin fractionations of ORW by Dang *et al.* (2010a, 2010b) indicate that hydrophobic acids are the main components of ORW NOM (i.e., 82%) and the transphilic acids and hydrophilic acids represent much smaller fractions (10.6% and 7.4%, respectively). SUVA, the specific ultraviolet absorbance, for ORW was 4.40 L $mg^{-1}m^{-1}$, confirming that hydrophobic acids (humic acids) constitutes a significant portion of the NOM in ORW. The large quantity of hydrophobic acids in ORW indicates that the foulants are predominantly negatively charged and can potentially foul membranes (Cheryan 1998). Several studies have reported that the hydrophobic fraction of NOM is primarily responsible for membrane fouling (Katsoufidou *et al.* 2005; Lee *et al.* 2008; Tian *et al.* 2013). The coagulation/sedimentation pretreatment achieved 51% TOC removal, a 75% reduction in the UV254 absorbance, and a 50% decrease in the SUVA, indicating that the humic fraction of the NOM was predominantly removed.

Effect of operating conditions on fouling rate

Figure 2(a) depicts the normalized specific flux decline for the runs with FTs of 15, 30, and 60 minutes with a BWT of 1 minute. All filtration experiments in this part of the study were conducted at a flux of 100 L/m^2h to observe fouling in a shorter period. A corresponding backwash flux of 250 L/m^2h was used based on the membrane manufacturer's recommendation. The sharp increases in the normalized specific flux at 0.25, 0.5, and 1 hour intervals are the result of the backwashing. These patterns are typical of those reported in the literature (MWH 2005; Pearce 2011). For a common BWT of 1 minute, the fouling rate decreased substantially with a decrease in FT from 60 to 15 minutes. However, the difference in fouling rate as FT decreased from 60 to 30 minutes was relatively small. According to Farahbakhsh *et al.* (2004), the mechanisms of NOM fouling on membrane systems may be divided into cake formation, surface adsorption-deposition, and adsorption-deposition in the membrane pores. The membrane permeability not recovered from hydraulic backwashes is thought to be primarily caused by adsorption fouling. Possible reasons for the

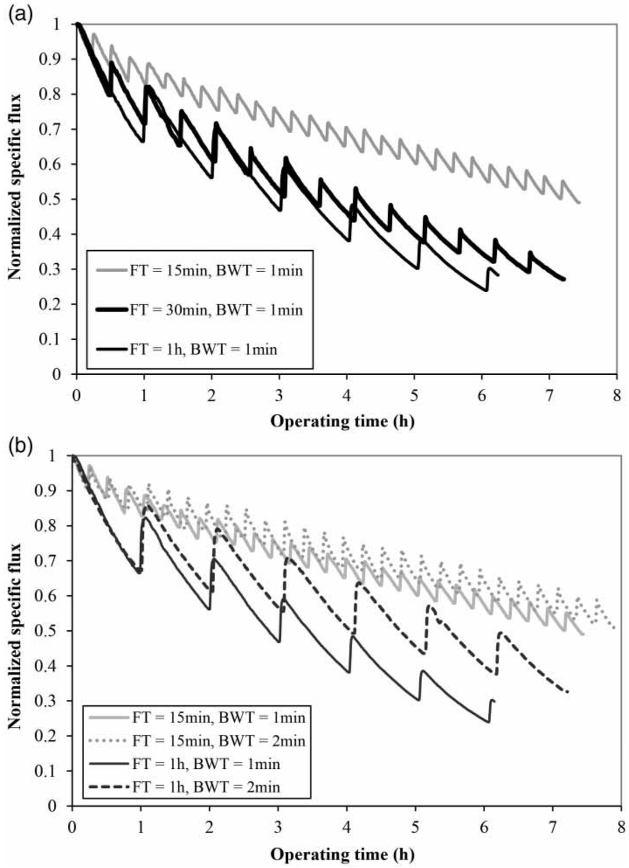

Figure 2 | Comparison of normalized specific flux decline: (a) for different FT; (b) for different BWT for constant flux of 100 L/m^2h for ORW.

observed results are that: (a) the fouling was probably caused by the adsorption of the mainly hydrophobic NOM on the membrane; (b) the magnitude of the sorption-related fouling increased from FT = 15 minutes to 30 minutes due to kinetic limitations; and (c) as the FT increased from 30 to 60 minutes, the impact decreased as the sorption sites were nearly exhausted. The large hydrophobic NOM concentration of ORW likely makes NOM adsorption a significant contributing fouling mechanism.

To avoid a very crowded graph, Figure 2(b) only presents the TMP development of the 15 minute and 1 hour filtration runs, with BWTs of 1 and 2 minutes. It shows that for short FTs, such as FT = 15 minutes, increasing the BWT had a small impact on the normalized flux decline, while for the 1 hour filtration cycles it had a larger impact and it became more significant with increasing operating time. It is believed that hydraulic backwashes help to remove the cake layer that forms on the surface of the membrane, and the effectiveness of the backwashing is expected to be a function of the BWT as well as the module configuration. For longer filtration cycles (FT = 1 hour) there would be greater cake accumulation on the membrane and presumably the longer backwash cycles are relatively more effective at removing more of this cake layer. Figure 2(b) indicates that to achieve optimal membrane backwashing, a sensitivity analysis of the operational variables is required. Also, because the impact of the operational variables appeared to increase with time, it is recommended that future studies incorporate longer filtration runs.

Flux decline patterns were compared for different operating fluxes, for a common BWT of 1 minute and a FT of 30 minutes (Figure 3). All backwash operations were performed at constant flux (two and a half times the filtration flux). The abscissa is the permeate volume treated per unit membrane area instead of operational time; this permits a comparison based on the same rate of foulant approach basis. Figure 3 shows that the fouling rate increased as the operating flux increased from 50 to 100 L/m^{2}h. The figure shows vast differences in the fouling rate between the low flux (50 L/m^{2}h) and high flux tests (100 L/m^{2}h). Therefore, this indicated that fouling rate is affected by more than just the rate of foulant approach to the membrane. A potential reason for this behavior is that higher fluxes create denser foulant cake layers, which would be more difficult to remove by backwashing.

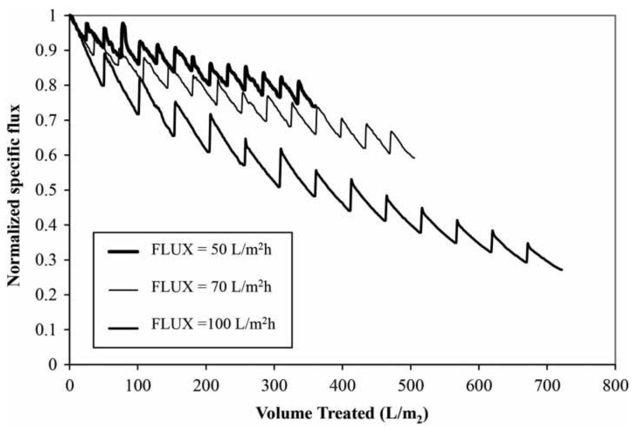

Figure 3 | Comparison of normalized specific flux decline for different operating flux values for FT of 30 minutes, BWT of 1 minute and backwash flux at 2.5 times the filtration flux for ORW.

These observations are consistent with the findings of Kim & DiGiano (2006) and with the backwash efficiencies presented in the next section. For scale-up the most relevant information from these tests (Figures 2 and 3) is that the pressure drop is high even for the lowest flux rate and a large fraction of the fouling is hydraulically irreversible. Accordingly, pretreatment is required before a sustainable flux can be identified. Demonstrating this without resorting to pilot-scale test demonstrates the usefulness of these tests.

Effect of operating conditions on backwash efficiency

For the 100 L/m^{2}h experiments, the filtration experiments demonstrated that backwash efficiency decreased with increasing FT, ranging from 85.2% for the 15 minute FT and 2 minute BWT to 63% for the 1 hour FT and 1 minute BWT (Table 2). These high backwash efficiency

Table 2 | Effects of experimental conditions on backwash efficiency

Flux (L/m^{2}h)	FT (min)	BWT (min)	Backwash efficiency (%)
100	15	1	81.5
	15	2	82.5
	30	1	71.0
	30	2	77.0
	60	1	63.0
	60	2	70.0
50	30	1	79.2
70	30	1	72.0
100	30	1	70.5

values seem to indicate that there was significant cake formation and that the backwashing was fairly effective. For the 15 minute filtration cycles increasing BWT from 1 minute to 2 minutes did not increase the backwashing efficiency substantially. However, as the FT lengthened to 30 minutes and 1 hour, the impact of BWT on backwashing efficiency became more pronounced. The lower η values for the 60 minute FT, indicated that the larger cake layer accumulated over the 60 minutes may be more difficult to clean (Kim & DiGiano 2006).

Table 2 also shows that for the 30 minute FT tests, increasing the permeate flux decreases the backwashing efficiency. The highest average backwash efficiency achieved was 79.2% for the 50 L/m^{2}h operating flux, while the lowest backwash efficiency obtained was 70.5% for the 100 L/m^{2}h operating flux. Operating at lower flux values proved to be beneficial, presumably since the cake layer seemed less rigidly attached, resulting in higher backwashing efficiency. The results again demonstrated that higher operating flux required frequent backwashing to adequately clear the accumulated cake layer.

Effect of operating conditions on NOM rejection

Due to the low filtrate volumes produced in these experiments, hourly composite samples were collected to have sufficient volume for turbidity, pH, TOC, and UV analyses. The presented results are the mean values from duplicate filtration experiments under the same operating conditions. The TOC rejections were very constant over the length of the filtration runs, ranging from 7 to 15%, which was expected given the membrane's nominal MWCO and molecular weight distribution of the NOM. These levels are also consistent with those reported in the literature (Pearce 2011). The TOC rejection increased slightly as FT decreased from 60 to 15 minutes (Figure 4); this pattern was the opposite of that expected if TOC removal by cake filtration/sorption was important. Potential mechanisms for these results are discussed at the end of the section. An increase in BWT from 1 minute to 2 minutes for the 15 minute filtration cycle showed a slightly improved TOC rejection. But for the longer filtration cycles, the TOC removals were statistically the same for the two different backwashing times. Given the small differences, this phenomenon requires further study.

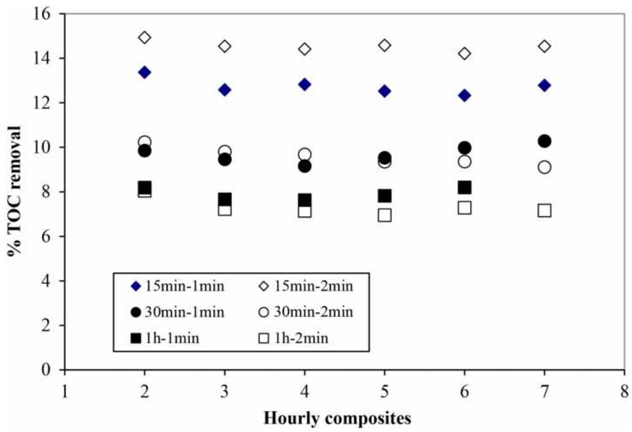

Figure 4 | TOC percentage rejection for different FT and BWT conditions for a constant flux of 100 L/m²h.

The tests demonstrated that the rejection of UVA-254, which is associated with the hydrophobic fraction of NOM, also increased as FT decreased from 60 to 15 minutes. An increase in BWT from 1 minute to 2 minutes did not increase the rejection of the humic content of NOM. Doubling the BWT from 1 minute to 2 minutes for the filtration cycle of 15 minutes did not increase UVA-254 rejection as it did the TOC rejection. This may be due to the competitive adsorption/desorption interactions between the various NOM fractions. In general, humic substances are more hydrophobic in nature and as such tend to be adsorbed to a higher degree (Croue et al. 1999), and the higher UVA-254 removal (12–22%) than TOC removal (7–15%) suggests that there is some NOM removal by adsorption. Adsorbed humic substances become firmly attached to the membrane and are more difficult to remove than the rest of the NOM. Therefore an increase in BWT from 1 minute to 2 minutes should not remove adsorbed humics, and lead to further humic substance rejection in subsequent filtration cycles. Although the differences in the percent rejection for the different filtration cycle lengths are small, they are statistically significant based on their 95% confidence limits.

The different flux tests showed that the TOC rejections were fairly constant over time and decreased from 15 to 7% as operating flux increased from 50 to 100 L/m^{2}h. Although the differences in the percent rejection for the different flux values are small, they are statistically significant given that 95% confidence levels do not overlap.

Size exclusion, pore adsorption and cake adsorption are the most commonly cited NOM removal mechanisms and they probably all occur to a certain extent in these experiments. Based on size exclusion alone, one would expect <8% rejection given the size of the NOM (i.e., 1–8% larger than 30 kDa) and the membrane's nominal MWCO (70 kDa). Thus there may be some removal by size exclusion but other mechanisms are also likely at play. Given the high hydrophobic NOM composition of ORW, sorption on the membrane pores, membrane surface or the cake layer could have a role. There could be greater size exclusion due to more blocked and narrowed pores caused by sorption in the pores, but the constant TOC removals with time seem to discount these as significant contributors. NOM adsorption is primarily irreversible in nature; the longer a membrane operates the greater the number of occupied adsorption sites leading to lower NOM rejections with each subsequent operating cycle. Thus, pore and membrane surface adsorption do not appear to be the controlling mechanism in this study. A third potential mechanism is removal by adsorption on the foulant cake. As FT or the flux increases, there should be greater cake accumulation on the membrane and presumably greater NOM removal by adsorption on the cake. As this also contradicts the observed results, cake adsorption does not appear to be the controlling mechanism. A further potential explanation for the TOC rejection pattern for the different flux experiments is that the higher flux could lead to greater NOM transport to the membrane surface as well as an increase in the volume of permeate throughput in a given time. This may lead to greater transport through the membrane, i.e., permeation drag, and lower NOM removals. The lower removals with increasing FT may also arise through the same mechanism. In conclusion, although we do not have direct proof about the NOM removal mechanisms, based on the above discussion it appears that: (a) size exclusion has a role and (b) the higher UV than TOC removals suggest that adsorption removal mechanisms also have a role in NOM removal. However, the removals cannot explain the decreasing removal pattern with increasing FT, this last behavior suggests that permeation drag also contributes to observed TOC removals.

Effect of pretreatment on membrane performance

Figure 5 shows the normalized specific flux decline versus operating time for raw ORW and coagulated/settled ORW. The pretreatment resulted in a substantially smaller decrease in the J_{NSF} during the first operating cycle, and the differences increased with subsequent cycles. The rate of flux decline is approximately five times greater for the raw ORW. The backwash efficiency for the chemically pretreated ORW was $93.42 + 0.78\%$ compared with $85.1 + 0.26\%$ for the best raw ORW run. The large impact of the pretreatment was expected given the high NOM content of raw ORW. Normally for high NOM waters, full-scale plants use pretreatment prior to membrane filtration; in this study, most runs were conducted with raw ORW to accelerate the fouling. Many researchers have also noticed similar significant improvements in J_{NSF} after chemical pretreatment of their respective source waters (Kim et al. 2005; Qin et al. 2006; Jung et al. 2006). Wiesner & Laîne (1996) attributed the reduction in fouling rate to the reduced pore plugging by the larger coagulated particulate matter in the raw water. Also, the decrease in SUVA indicates that a greater portion of the hydrophobic fraction of NOM was removed by the pretreatment. With less NOM adsorption, the backwash efficiency increased. Thus the bench-scale hollow fiber system clearly help to demonstrate the benefit of pretreatment and it can be used to evaluate alternative pretreatment strategies. Prior to scale-up, 3–4 day-long bench-scale tests should be performed using different permeate fluxes, to establish the sustainable flux for the pretreated

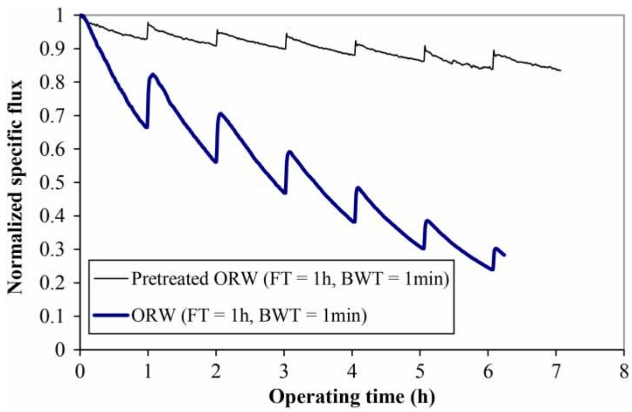

Figure 5 | Impact of pretreatment on the normalized flux at a flux of 100 L/m^2/h.

water, that is, the flux that minimizes fouling while maintaining reasonable water production.

Summary of experimental results

For the membrane filtration of the raw ORW samples a number of observations can be made about the system/membrane/water combination. (1) For a common BWT, the fouling rate decreased substantially by a decrease in FT; BWT was not as significant as FT but became more significant as the filtration cycle length increased. (2) Backwash efficiency increased as FT decreased; BWT did not significantly affect the backwash efficiency with the exception of the 1 hour FT. (3) As expected for UF systems, the NOM rejection was low and the hydrophobic fraction of NOM was removed to a higher extent, suggesting that NOM adsorption had a role in its removal. The rejection levels decreased slightly with increasing FT and permeate flux. (4) Higher operating fluxes increased the rate of approach of foulants to the membrane surface. However, the fouling rate exceeded the rate of approach indicating that the higher fluxes also impact other potentially important factors such as the cake characteristics. (5) The higher fouling rate resulted in a slight decrease in NOM rejection. It is speculated that it was caused by permeate drag. Backwash efficiency also decreased with increasing operating flux. (6) As expected, pretreatment resulted in a substantially smaller fouling rate and higher backwash efficiency. Thus for the treatment of ORW, coagulation pretreatment is highly recommended.

Modeling of membrane fouling

Many studies have attempted to determine the dominant mechanisms responsible for membrane fouling, and frequently models based on constant flow rate blocking laws were applied to the experimental data. There are four single mechanism blocking law models: cake, intermediate, complete, and standard blocking (Suarez & Veza 2000; Liu & Kim 2008). It may not be very realistic to assume that only one blocking law mechanism is dominant at any given time. Therefore, Bolton *et al.* (2006) developed five new models, each of which combined two single blocking laws. All nine models (four single and five combined mechanisms) were applied to our experimental data to obtain predicted TMP values over time. The difference between the measured and predicted TMP was squared, summed, and minimized by changing the fitted parameters using Microsoft Excel's solver. Residual mean square (RMS) was calculated for comparison between experiments, to compensate for the fact that the combined mechanism models have two adjustable parameters while the single mechanism models have one (MacBerthouex & Brown 2002).

The first, middle, and the last filtration cycles in each of six experiments were analyzed using the blocking law models. They were able to simulate the data quite well, and Figure 6 shows an example of these simulations. Table 3(a) shows compilations of the RMS values for the experiments and models. The combined models were omitted because only in one of the 18 cycle/run simulations did a dual mechanism model yield a significantly better simulation than the best-fitting single mechanism model. The model with the lowest RMS value for each simulation is shown in bold; these are the best fitting models for the particular simulation. The key results from these tables are as follows. First, for most operating conditions, two or more of the models yielded very similar low RMS values, making it very difficult to identify the best fitting model. Second, during the first filtration cycle (in which the backwashing is not yet a factor) there is no individual mechanism that appears to control the fouling. Surprisingly, this applies for the runs with the same FT as they have very similar J_{NSF} profiles, as shown in Figure 2(b). Third, for the

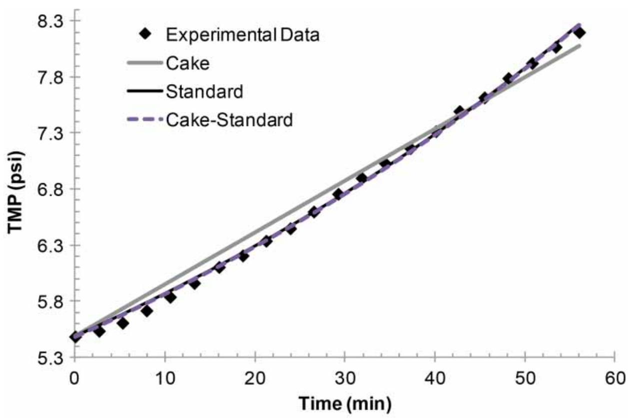

Figure 6 | Comparison of cake, standard, and cake-standard models for the 1 hour 1 minute first cycle experiment.

Table 3 | RMSs for all models and experiments

(a) RMSs – first cycle

Model	Raw 15m1m	Raw 15m2m	Raw 30m1m	Raw 30m2m	Raw 1hr1m	Raw 1hr2m
Cake	***0.0173****	0.0131	0.0388	***0.0541***	0.1030	***0.0219***
Intermediate	0.0194	0.0124	0.0258	0.0813	***0.0493***	0.0784
Complete	0.0213	0.0131	***0.0163***	0.1121	0.0622	0.1552
Standard	0.0203	***0.0126***	0.0202	0.0964	0.0416	0.1156

(b) Best fitting model

Cycle	15m1m	15m2m	30m1m	30m2m	1hr1m	1hr2m
First cycle	Cake	Standard	Complete	Cake	Intermediate	Cake
Middle cycle	Complete	Cake	Cake	Complete	Standard	Complete
Last cycle	Cake	Cake	Cake	Intermediate	Intermediate	Standard

*In bold the lowest RMS value, i.e. the best fitting model.

middle and last filtration cycles, the best fitting models also vary from one operating condition to the next (Table 3(b)). Fourth, for every set of operating conditions, the best fitting models tend to change as the filtration proceeds from the first to the last cycle; these changes do not seem to fit a clear pattern (Table 3(b)). Accordingly, this modeling approach does not seem well suited for identifying the controlling fouling mechanisms for this type of filtration system and these models should not be used to predict long-term membrane performance.

The reason for assessing the data at the beginning, middle, and end of the experiment was to determine if fouling mechanism dominance changed over time, as the experiment progressed. While for the first cycle the cake filtration model yielded the lowest RMS for half of the six runs (Table 3(b)), for the later cycles (Table 3(b)) this was not necessarily the case. As the experiment progressed with time (i.e., more cycles are performed), it was expected that standard blocking would be less dominant in the later stages of the experiment (Bolton *et al.* 2006; Huang *et al.* 2008). Based on this hypothesis, the standard blocking model should have fitted the experimental data better for the first filtration cycle than the middle and last filtration cycles; however, this did not appear to be the case. This may be partly because there are TMP variabilities from one operational cycle to the next and because the backwash efficiencies are not uniform throughout. Given that for multi-cycle filtration tests, like those conducted in this study, modeling individual filtration cycles using the blocking law models does not appear to yield a logical progression of mechanisms, and this approach is not recommended. All of this points to the difficulty of modeling the complex membrane fouling processes when there are no measurements to independently quantify the role of each mechanism. Furthermore, the J_{NSF} profiles change with time indicating that the nature of the fouling changes as the membrane operates longer. Fouling is extremely complex.

CONCLUSIONS

The constant flux UF bench-scale system built for this study incorporated automated filtration and backwash cycles and mimicked the performance of full-scale systems. As such it is a convenient tool to assess the impact of operating conditions on membrane fouling and of alternative pretreatment options. Although not demonstrated in this manuscript, these bench-scale systems can also be used to evaluate alternative membrane types, and alternative chemical membrane cleaning options. The development of the new system yielded the following findings. First, it was found that it was difficult to maintain a constant permeate flowrate during the first minutes after the backwash step; a good computer control scheme was required. Second, electronic flowmeters are not recommended for this type of system because they are highly susceptible to bubbles that seem to be generated by the switching of the solenoid valves. Third, the length of backwash waste lines should be minimized to eliminate carryover of foulants into the next filtration cycle.

The UF membrane filtration results of raw ORW, that is typical of Northern Canadian waters, using different permeate fluxes, and filtration and backwash cycles' durations yielded many typical patterns observed in full-scale systems. Although it was expected, the most practical results of the tests is that ORW should be pretreated prior to membrane filtration. As the NOM characteristics vary with the water source, some differences in performance may occur. For this particular water/membrane combination, one of the exceptions observed was that the percent NOM removal decreased slightly for the higher NOM loading rates; it was speculated that the NOM removal was influenced by permeate drag.

The single mechanism fouling models described fouling relatively well, when the fouling data during the first, middle, and last filtration cycles of the six runs was modeled. As several models simulated the data well and the best fitting models varied with different operating conditions, no conclusions can be made about controlling fouling mechanisms. In addition, for multi-cycle filtration tests, like those conducted in this study, modeling individual filtration cycles using the blocking law models does not appear to yield a consistent logical progression of fouling mechanisms, thus this approach is not recommended. Accordingly, these models should not be used to predict long-term membrane performance and are of little practical value for systems involving many short filtration cycles.

ACKNOWLEDGEMENTS

This research was supported by the Natural Sciences and Engineering Research Council of Canada.

REFERENCES

APHA, AWWA & WEF 1998 *Standard Methods for the Examination of Water and Wastewater*, 20th edn. American Public Health Association/American Water Works Association/Water Environment Federation, Washington, DC, USA.

Bolton, G., LaCasse, D. & Kuriyel, R. 2006 Combined models of membrane fouling: development and application to microfiltration and ultrafiltration of biological fluids. *J. Membr. Sci.* **277**, 75–84.

Chellam, S., Jacangelo, J. & Bonacquisti, T. 1998 Modeling and experimental verification of pilot-plant scale hollow fiber, direct flow microfiltration with periodic backwashing. *Environ. Sci. Technol.* **32**, 75–81.

Cheryan, M. 1998 *Ultrafiltration and Microfiltration Handbook*. Technomic Publishing Co., Lancaster, PA, USA.

Croue, J.-P., Korshin, G. V. & Benjamin, M. 1999 *Characterization of Natural Organic Matter in Drinking Water*. AWWA Research Foundation, Denver, CO, USA.

Dang, H. T., Rana, D., Narbaitz, R. M. & Matsuura, T. 2010a Key factors affecting the manufacture of hydrophobic ultrafiltration membranes for surface water treatment. *J. App. Poly. Sci.* **116**, 2626–2637.

Dang, H. T., Narbaitz, R. M. & Matsuura, T. 2010b Evaluation of apparatus for membrane cleaning tests. *J. Environ. Eng.* **136**, 1161–1170.

Farahbakhsh, K., Svreck, C., Gust, R. K. & Smith, D. W. 2004 A review of the impact of chemical pretreatment on low-pressure water treatment membranes. *J. Environ. Eng. Sci.* **3**, 237–253.

Heijman, S., Gijsbertsen, A. & Amy, G. 2005 Water quality test for dead-end ultrafiltration. In *AWWA WQTC Conference, Quebec, Canada*, pp. 1–7.

Huang, H., Young, T. A. & Jacangelo, J. G. 2008 Unified membrane fouling index for low pressure membrane filtration of natural waters: principles and methodology. *Environ. Sci. Technol.* **42**, 714–720.

Jacangelo, J. G., Laîne, J., Cummings, E. W., Deutschmann, A., Malleviale, J. & Wiesner, M. R. 1994 *Evaluation of Ultrafiltration Membrane Pretreatment and Nanofiltration of Surface Waters*. AWWA Research Foundation, Denver, CO, USA.

Jung, C.-W., Son, H.-J. & Kang, L.-S. 2006 Effects of membrane material and pretreatment coagulation on membrane fouling: fouling mechanism and NOM removal. *Desalination* **197**, 154–164.

Katsoufidou, K., Yiantsios, S. G. & Karabelas, A. J. 2005 A study of ultrafiltration membrane fouling by humic acids and flux recovery by backwashing: experiments and modeling. *J. Membr. Sci.* **266**, 40–50.

Kim, J. & DiGiano, F. 2006 A two-fiber, bench-scale test of ultrafiltration (UF) for investigation of fouling rate and characteristics. *J. Membr. Sci.* **271**, 194–204.

Kim, S.-H., Moon, S.-Y., Yoon, C.-H., Yim, S.-K. & Cho, J.-W. 2005 Role of coagulation in membrane filtration of wastewater for reuse. *Desalination* **173**, 301–307.

Lee, E. K., Chen, V. & Fane, A. 2008 Natural organic matter (NOM) fouling in low pressure membrane filtration – effect of membranes and operation modes. *Desalination* **218**, 257–270.

Liu, Q.-F. & Kim, S.-H. 2008 Evaluation of membrane fouling models based on bench-scale experiments: a comparison between constant flowrate blocking laws and artificial neural network (ANNs) model. *J. Mem. Sci.* **310**, 393–401.

Mac Berthouex, P. & Brown, L. C. 2002 *Statistics for Environmental Engineers*, 2nd edn. CRC Press, Boca Raton, FL, USA.

Mosqueda-Jimenez, D. B., Narbaitz, R. M. & Matsuura, T. 2004 Membrane fouling test: apparatus evaluation. *J. Environ. Eng.* **130**, 90–99.

MWH 2005 *Water Treatment Principles and Design*. J. Wiley & Sons, Inc., Hoboken, NJ, USA.

Nakatsuka, S., Nakate, I. & Miyano, T. 1996 Drinking water treatment by using ultrafiltration hollow fiber membranes. *Desalination* **106**, 55–61.

Nguyen, H.-A., Narbaitz, R. M. & Matsuura, T. 2007 Impacts of hydrophilic membrane additives on the ultrafiltration of river water. *J. Environ. Eng.* **133**, 515–522.

Pearce, G. K. 2011 *UF/MF Membrane Water Treatment: Principles & Design*. TechnoBiz Commun., Bangkok, Thailand.

Qin, J. J., Oo, M. H., Kekre, K. A., Knops, F. & Miller, P. 2006 Reservoir water treatment using hybrid coagulation-ultrafiltration. *Desalination* **193**, 344–349.

Suarez, J. A. & Veza, J. M. 2000 Dead-end microfiltration as advanced treatment for wastewater. *Desalination* **127**, 47–58.

Tian, J., Ernst, M., Cui, F. & Jekel, M. 2013 Effect of different cations on UF membrane fouling by NOM fractions. *Chem. Eng. J.* **223**, 547–555.

Touffet, A., Baron, J., Welte, B., Joyeux, M., Teychene, B. & Gallard, H. 2015 Impact of pretreatment conditions and chemical ageing on ultrafiltration membrane performances. Diagnostic of a coagulation/adsorption/filtration process. *J. Membr. Sci.* **489**, 284–291.

Wiesner, M. R. & Laîne, J. M. 1996 Coagulation and membrane separation. In: *Water Treatment Membrane Processes* (J. Mallevialle, P. E. Odendaal & M. R. Wiesner, eds). McGraw-Hill, New York, USA, pp. 16.1–16.11.

Wray, H. E., Andrews, R. C. & Berube, P. R. 2014 Ultrafiltration organic fouling control: comparison of air-sparging and coagulation. *J. Amer. Water Works Assoc.* **106** (2), 76–85.

Yin, Z., Tarabara, V. V. & Xagoraraki, I. 2015 Human adenovirus removal by hollow fiber membranes: Effect of membrane fouling by suspended and dissolved matter. *J. Membr. Sci.* **482**, 120–127.

Yu, W. & Graham, N. J. D. 2015 Performance of an integrated granular media – Ultrafiltration membrane process for drinking water treatment. *J. Membr. Sci.* **492**, 164–172.

Zularisam, A., Ismail, A. & Salim, R. 2006 Behaviours of natural organic matter in membrane filtration for surface water treatment – a review. *Desalination* **194**, 211–231.

First received 5 October 2015; accepted in revised form 3 February 2016. Available online 2 March 2016